NATIONAL AERONAUTICS AND SPACE ADMINISTRATION

Technical Report 32-1502

Parametric Study of the Performance Characteristics and Weight Variations of Large-Area Roll-Up Solar Arrays

J. V. Coyner, Jr.
R. G. Ross, Jr.

JET PROPULSION LABORATORY
CALIFORNIA INSTITUTE OF TECHNOLOGY
PASADENA, CALIFORNIA

December 15, 1970

NATIONAL AERONAUTICS AND SPACE ADMINISTRATION

Technical Report 32-1502

Parametric Study of the Performance Characteristics and Weight Variations of Large-Area Roll-Up Solar Arrays

J. V. Coyner, Jr.
R. G. Ross, Jr.

JET PROPULSION LABORATORY
CALIFORNIA INSTITUTE OF TECHNOLOGY
PASADENA, CALIFORNIA

December 15, 1970

Prepared Under Contract No. NAS 7-100
National Aeronautics and Space Administration

Preface

The work described in this report was performed by the Engineering Mechanics Division of the Jet Propulsion Laboratory.

Contents

I. Introduction 1

II. Optimum Boom and Blanket Tension Analysis 2

III. Support Structure Analysis 4

IV. Solar Array Parametric Study 7

V. Use of Parametric Curves 8

VI. Conclusion 12

References 13

Appendix A. Parametric Plots 14

Appendix B. Elemental Stiffness and Consistent Mass Matrices for Blanket and Beam Elements 22

Tables

1. Geometric scale factor and stress-level relationships 6
2. Scale-factor solutions for individual components 6

Figures

1. Deployed array 1
2. Deployed array mode shapes 2
3. Typical plot of frequency vs blanket tension 2
4. Computer program flow chart 3
5. Typical finite-element models 3
6. Dependence of component weights on natural frequency and array aspect ratio for a typical 250-ft^2 BI-STEM boom array 8
7. Optimum aspect ratio for any size array as a function of deployed natural frequency 8
8. Typical dependence of power-to-weight ratio on deployed natural frequency for various array widths 9
9. Optimum boom stiffness and blanket tension vs deployed natural frequency and blanket area for a typical array width 10

Contents (contd)

Figures (contd)

10. Variation in array length with deployed natural frequency caused by increase in boom length and actuator width with increasing boom stiffness for a typical steel BI-STEM boom with $D/t = 200$ and 80% efficiency 11

11. Boom diameter and boom-actuator width as a function of bending stiffness for a steel BI-STEM element (assuming 80% efficiency) 11

12. Weight per foot vs bending stiffness for a steel BI-STEM boom element (assuming 80% efficiency) 11

13. Dependence of solar-array efficiency on blanket weight per unit area for a typical 8.25-ft-wide, 250-ft² area, 10-W/ft² output, steel BI-STEM boom array 12

14. Dependence of optimum (minimum) boom stiffness on blanket weight per unit area for a typical 8.25-ft wide, 250-ft² area, 10-W/ft² output, steel BI-STEM boom array 12

A-1. Optimum aspect ratio for any size array as a function of deployed natural frequency 15

A-2. Dependence of power-to-weight ratio upon deployed natural frequency for various array widths (100-ft² blanket area) 15

A-3. Dependence of power-to-weight ratio upon deployed natural frequency for various array widths (150-ft² blanket area) 15

A-4. Dependence of power-to-weight ratio upon deployed natural frequency for various array widths (200-ft² blanket area) 15

A-5. Dependence of power-to-weight ratio upon deployed natural frequency for various array widths (250-ft² blanket area) 16

A-6. Dependence of power-to-weight ratio upon deployed natural frequency for various array widths (300-ft² blanket area) 16

A-7. Dependence of power-to-weight ratio upon deployed natural frequency for various array widths (350-ft² blanket area) 16

A-8. Dependence of power-to-weight ratio upon deployed natural frequency for various array widths (400-ft² blanket area) 16

A-9. Optimum boom stiffness for a 4-ft-wide array 17

Contents (contd)

Figures (contd)

A-10. Optimum boom stiffness for a 6-ft-wide array 18

A-11. Optimum boom stiffness for an 8.25-ft-wide array 19

A-12. Optimum boom stiffness for a 12-ft-wide array 20

A-13. Array length vs deployed natural frequency and blanket area for a 4-ft-wide array 21

A-14. Array length vs deployed natural frequency and blanket area for a 6-ft-wide array 21

A-15. Array length vs deployed natural frequency and blanket area for an 8.25-ft-wide array 21

A-16. Array length vs deployed natural frequency and blanket area for a 12-ft-wide array 21

B-1. Rectangular membrane finite element 23

B-2. Beam column finite element 23

Abstract

An analysis has been conducted to determine the relationships between the performance characteristics (power-to-weight ratio, blanket tension, structural member section dimensions, and resonant frequencies) of large-area roll-up solar arrays of the single-boom, tensioned-substrate design. The study includes the determination of the size and weight of the base structure supporting the boom and blanket and the determination of the optimum width, blanket tension, and deployable boom stiffness needed to achieve the minimum-weight design for a specified frequency for the first mode of vibration. A computer program has been used to generate a set of plots that provide optimum structural sizing and estimated weights for arrays with blanket areas ranging from 100 to 400 ft^2 and for first-mode natural frequencies ranging from 0.03 to 0.7 Hz. Use of these plots enables a quick evaluation of the potential merits of a proposed roll-up array.

Parametric Study of the Performance Characteristics and Weight Variations of Large-Area Roll-Up Solar Arrays

I. Introduction

In recent years, considerable emphasis has been placed on the development of large-area solar arrays with high power-to-weight ratios and small packaging volumes. One of the concepts currently being developed is the single-boom roll-up array shown in Fig. 1.

The design consists of two flexible-cell blankets tensioned between spacecraft-mounted storage drums and a leading-edge beam. The array is erected by a deployable boom that is connected between the leading-edge beam and its supporting structure on the spacecraft.

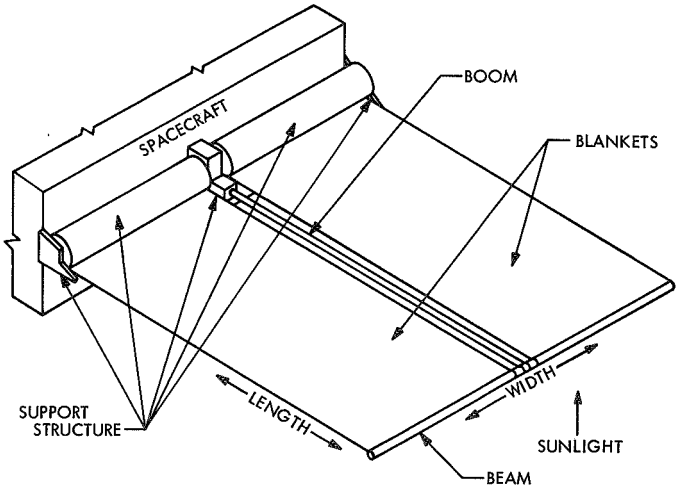

Fig. 1. Deployed array

In studying potential applications for this design, one must predict the performance characteristics of arrays of widely varying sizes and natural frequencies. Because of the complex nature of the relationship between the size of the array, its first-mode natural frequency, and its structural parameters, it is difficult to predict the performance characteristics of arrays significantly different from the engineering prototype. To help solve this problem, a computer routine was programmed to calculate the optimum size for structural members and the optimum blanket tension for an array that is to have a given electrical power output and a specified lowest deployed natural frequency. The program is composed of two basic parts: (1) an analysis of the deployable boom and array blanket and (2) an analysis and sizing of the base structure supporting the boom and array blankets.

After the computer program had been developed, a parametric study was conducted to provide approximate structural sizing and estimated weights for arrays with blanket areas ranging from 100 to 400 ft^2, widths ranging from 4 to 12 ft, and first-mode natural frequencies ranging from 0.03 to 0.7 Hz. These data, which are presented in graphical form, should provide enough information for preliminary configuration studies.

Although the results presented apply only to the single-boom, two-drum design, the computer program is so designed that adaptation to other configurations can be accomplished simply by adding and removing certain subroutines. This will allow analysis of new design concepts without complete revision of the existing program.

II. Optimum Boom and Blanket Tension Analysis

If the width of the array and the power output per unit area of blanket are specified, the length (and thus the size) of the array is fixed by the total electrical power output required. Because the weight of the cell blanket and support structure is essentially fixed for an array of a given size, the relationship between total weight and deployed natural frequency is almost entirely controlled by the weight of the deployment boom. This implies that, when the size of the array is specified, the optimum array for a specific lowest deployed natural frequency can be defined as that with the lightest boom.

Because there are two possible first-vibration modes for a deployed array (Fig. 2), the cross-sectional size (and thus the weight) of the boom is determined by the following requirement: the boom must have sufficient stiffness to maintain the first-bending frequency equal to or greater than the required minimum frequency while loaded by sufficient blanket tension to maintain the first-torsion frequency at or above the minimum. Figure 3 shows the variation in first-bending and first-torsion frequencies as a function of the blanket tension for a single-boom array of the type under investigation. As is shown in this figure, the optimum tension for a particular boom stiffness has been found to occur when the first symmetric and antisymmetric frequencies are equal. This tension yields the lightest boom for a particular lowest deployed natural frequency.

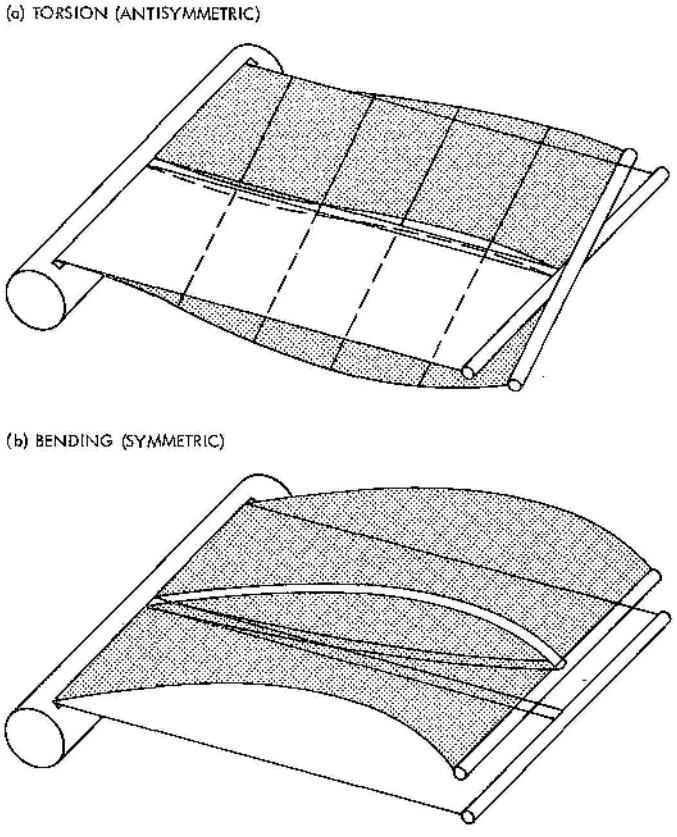

Fig. 2. Deployed array mode shapes

The natural frequencies of the array being nonlinear functions of the blanket tension, the roll-up array performance program uses an efficient root-finding routine to determine the optimum blanket tension as defined by F (tension) = (symmetric frequency − antisymmetric frequency) = 0.

Each evaluation of the function F requires the calculation of the natural frequencies of the combined tensioned-blanket/axial-loaded boom system that makes up the deployed array.

Once the optimum tension for a given boom stiffness has been determined, a second root-finding routine is used to determine the boom stiffness that results in the lowest deployed frequency being equal to the desired minimum deployed natural frequency; i.e., F (boom stiffness) = (first-mode frequency − required frequency) = 0. A flow chart of the complete iteration sequence used in the program is shown in Fig. 4.

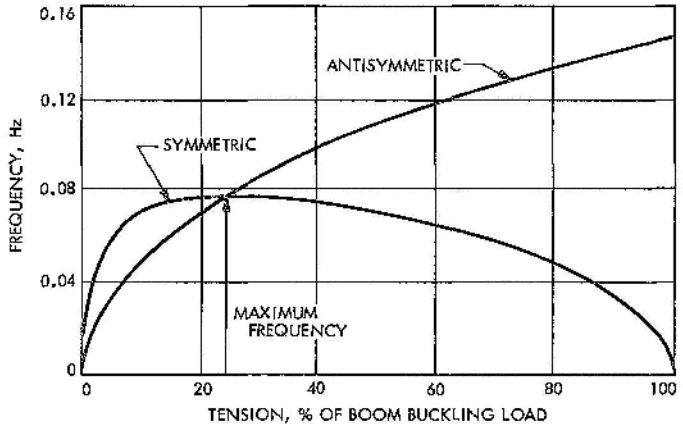

Fig. 3. Typical plot of frequency vs blanket tension

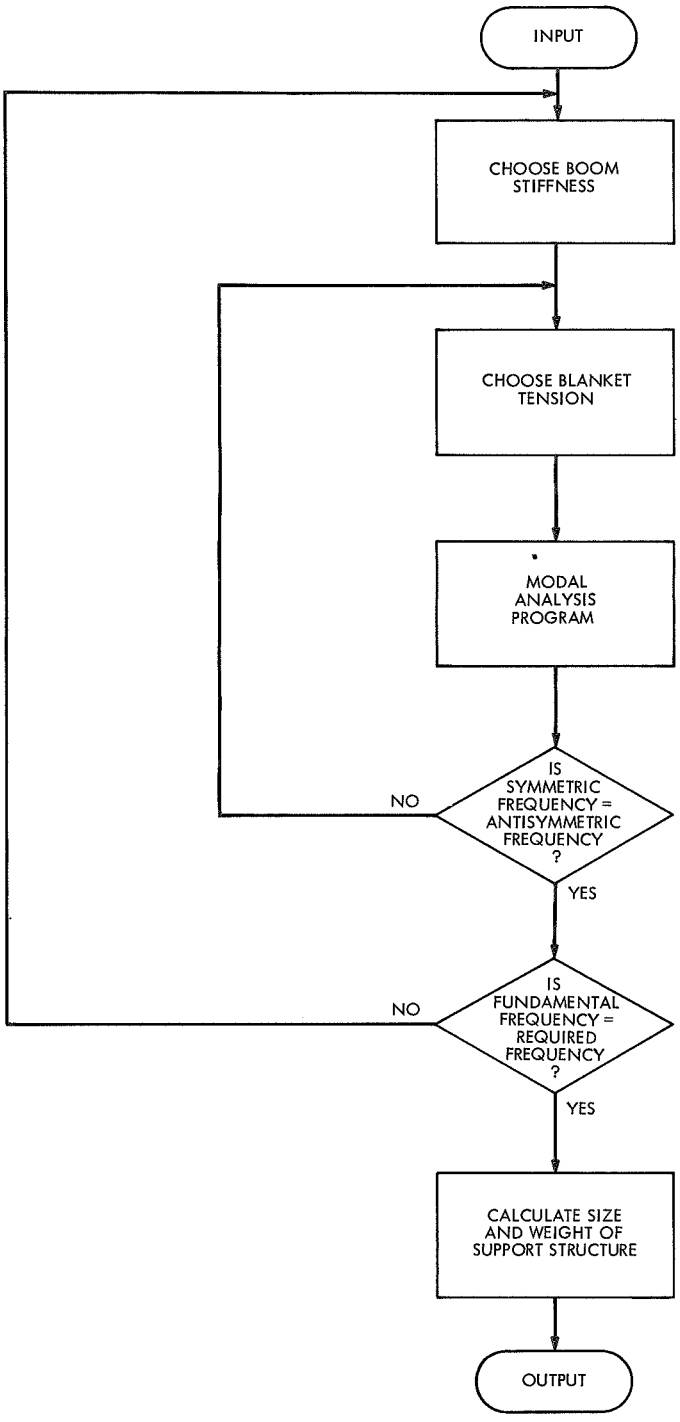

Fig. 4. Computer program flow chart

The modal analysis of the deployed solar array is based on a multi-degree-of-freedom, finite-element representation of the boom, beam, and blanket components, as shown in Fig. 5. Each blanket is modeled by 10 rectangular finite elements, which describe the out-of-plane stiffness caused by the imposed blanket tension. The boom and beam components are similarly modeled by standard beam-column elements, which describe both the bending stiffness and the geometric stiffness caused by the axial preload.* Although the blanket bending stiffness is neglected in the above analysis, more sophisticated 250-degrees-of-freedom analyses, which include the bending stiffness, have shown that the simple model leads to less than 1% errors in the first-mode frequencies.

The stiffness and mass matrices for the overall array are developed by combining the element stiffness and consistent mass matrices for the elements described above. The generation procedure allows for the following arbitrary parameters:

(1) Array length.

(2) Array width.

(3) Blanket weight/unit area.

(4) Boom weight/unit length.

(5) Beam weight/unit length.

(6) Boom stiffness.

(7) Beam stiffness.

(8) Blanket tension.

After initialization of the above parameters by the root-finding routines, the natural frequencies of the array are determined by solution of the usual eigenvalue problem with a very fast Q–R algorithm.

*The elemental stiffness and consistent mass matrices for the blanket and beam elements were derived by use of the techniques of Martin (Ref. 1), and are given in Appendix B.

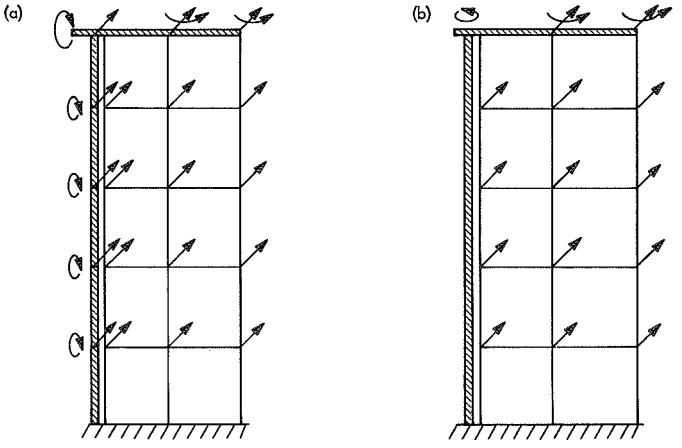

Fig. 5. Typical finite-element models: (a) symmetric, (b) antisymmetric

III. Support Structure Analysis

The support structure analysis uses scaling equations to extrapolate the size and weight of the support-structure components of a proposed array from those of a baseline design. The configuration used as the baseline for this analysis is the 8.25-ft wide, 250-ft^2 engineering prototype described in Ref. 2. Essentially, a dimensional-analysis approach was taken to determine the scale factors that are applied to the structural elements when design conditions change. The total weight W_1 of the reference array is broken down into 12 components:

$$W_1 = W_{bo1} + W_{s1} + W_{c1} + W_{b1} + W_{ss1} + W_{es1} + W_{cs1} + W_{be1} + W_{a1} + W_{ns1} + W_{bkt1} + W_{neg1} \quad (1)$$

where

W_{bo1} = weight of boom (determined by modal analysis program)

W_{s1} = weight of storage drum shell

W_{c1} = weight of end caps on storage drum shell

W_{b1} = weight of bearings

W_{ss1} = weight of support shaft

W_{es1} = weight of end supports

W_{cs1} = weight of center support

W_{be1} = weight of beam (leading-edge member)

W_{a1} = weight of boom actuator

W_{ns1} = weight of nonstructural material

W_{bkt1} = weight of solar-array blanket

W_{neg1} = weight of NEG'ATOR spring-mechanism hardware (constant-force spring)

(Subscript 1 refers to the reference array; the alphabetic subscripts refer to the structural components.)

The weight of a second array—differing from the reference array in geometry, material properties, and applied inertial loads—can be broken down in a similar manner:

$$W_2 = W_{bo2} + W_{s2} + W_{c2} + W_{b2} + W_{ss2} + W_{es2} + W_{cs2} + W_{be2} + W_{a2} + W_{ns2} + W_{bkt2} + W_{neg2} \quad (2)$$

The ratio $W_t = W_2/W_1$ can be written as

$$W_t = \frac{W_2}{W_1} = \frac{W_{bo2}W_{bo1}}{W_{bo1}W_1} + \frac{W_{s2}}{W_{s1}}\frac{W_{s1}}{W_1} + \frac{W_{c2}}{W_{c1}}\frac{W_{c1}}{W_1} + \frac{W_{b2}}{W_{b1}}\frac{W_{b1}}{W_1} + \frac{W_{ss2}}{W_{ss1}}\frac{W_{ss1}}{W_1} + \frac{W_{es2}}{W_{es1}}\frac{W_{es1}}{W_1} + \frac{W_{cs2}}{W_{cs1}}\frac{W_{cs1}}{W_1} + \frac{W_{be2}}{W_{be1}}\frac{W_{be1}}{W_1} + \frac{W_{a2}}{W_{a1}}\frac{W_{a1}}{W_1} + \frac{W_{ns2}}{W_{ns1}}\frac{W_{ns1}}{W_1} + \frac{W_{bkt2}}{W_{bkt1}}\frac{W_{bkt1}}{W_1} + \frac{W_{neg2}}{W_{neg1}}\frac{W_{neg1}}{W_1} \quad (3)$$

where W_{bo1}/W_1, W_{s1}/W_1, W_{c1}/W_1, etc., are the fractions of the total weight of the reference array contributed by the individual components. A simplified notation is used to refer to the ratios of the weights of the components, $W_{bo2}/W_{bo1} = W_{bo}$, $W_{s2}/W_{s1} = W_s$, $W_{c2}/W_{c1} = W_c$, etc.

Geometric scale factors are introduced to define the change in size of the components, and relationships are then established between these geometric scale factors and the ratio of stresses in the components. The scale factors used are as follows:

λ^{so} = structural section overall scale factor

λ^{st} = structural section material thickness scale factor

λ_h = blanket width scale factor

λ'_h = total array width scale factor

λ_v = blanket length scale factor

λ_t = ratio of blanket tension of array 2 to that of array 1

λ_{acc} = ratio of launch-acceleration loading of array 2 to that of array 1

λ_{dia} = ratio of boom diameter of array 2 to that of array 1

λ_{ves} = ratio of total diameter of combined storage drum shell and rolled blanket of array 2 to that of array 1

Because only one acceleration load factor λ_{acc} relates the acceleration loadings in the three orthogonal directions (parallel to storage drum, perpendicular to storage drum and in plane of blanket, and perpendicular to storage drum and normal to plane of blanket), this factor is an average of these three orthogonal acceleration factors.

By expressing the weight ratios in terms of material densities and volumes, and by expressing the volumes in terms of the scale factors, Eq. (3) becomes

$$W_t = \frac{W_{bo1}}{W_1}[W_{bo}] + \frac{W_{s1}}{W_1}\left[\frac{\rho_{s2}}{\rho_{s1}}(\lambda_s^{so}\,\lambda_s^{st}\,\lambda_h)\right] + \frac{W_{c1}}{W_1}\left[\frac{\rho_{c2}}{\rho_{c1}}(\lambda_s^{so})(\lambda_c^{st})^2\right] + \frac{W_{b1}}{W_1}\left[\frac{\rho_{b2}}{\rho_{b1}}(\lambda_{ss}^{so})^2\right] + \frac{W_{ss1}}{W_1}\left[\frac{\rho_{ss2}}{\rho_{ss1}}(\lambda_{ss}^{so}\lambda_{ss}^{st}\lambda_h)\right] + \frac{W_{es1}}{W_1}\left[\frac{\rho_{es2}}{\rho_{es1}}(\lambda_{es}^{so}\,\lambda_{es}^{st}\,\lambda_{ves})\right] + \frac{W_{cs1}}{W_1}\left[\frac{\rho_{cs2}}{\rho_{cs1}}(\lambda_{dia}\,\lambda_{cs}^{st}\,\lambda_{ves})\right] + \frac{W_{be1}}{W_1}\left[\frac{\rho_{be2}}{\rho_{be1}}(\lambda_{be}^{so}\lambda_{be}^{st}\lambda_h')\right] + \frac{W_{a1}}{W_1}\left[\frac{\rho_{a2}}{\rho_{a1}}(\lambda_{dia}\,\lambda_a^{st}\,\lambda_v^{1/2})\right] + \frac{W_{ns1}}{W_1}\left[\frac{\rho_{ns2}}{\rho_{ns1}}(\lambda_h\lambda_v)\right] + \frac{W_{bkt1}}{W_1}\left[\frac{\rho_{bkt2}}{\rho_{bkt1}}\quad\lambda_h\lambda_v\right] + \frac{W_{neg1}}{W_1}\left[\frac{\rho_{neg2}}{\rho_{neg1}}(\lambda_t)^{1/2}\right] \tag{4}$$

where ρ is the material density of the components, the subscripts to the geometric scale factors and densities indicate the structural components to which they refer, and the superscripts *st* and *so* indicate whether the scale factor refers to thickness or to overall size, respectively.

Relationships are then established between the geometric scale factors in Eq. (4) and the ratios of stresses of the components of the structure. This must be done individually for each of the components sized by stress and load levels, and the results then substituted into Eq. (4). Some components, however, are not sized by stress and load levels.

The ratio of the boom weights W_{bo} is determined by the modal analysis program. The NEG'ATOR spring-mechanism weight is a function of blanket tension. Blanket weight is a function of λ_h and λ_v. Nonstructural hardware is also assumed to be a function of λ_h and λ_v, and bearing size is a function of support-shaft size.

The derivation of the relationships for the storage drum shell will be considered as a typical example. For inertial loading, beam-bending moments are related by

$$\frac{M_2}{M_1} = \lambda_{acc}\lambda_h W_{bs} \tag{5}$$

where $W_{bs} = (W_{bkt2} + W_{s2})/(W_{bkt1} + W_{s1})$. The corresponding ratio of shell maximum bending stresses is

$$\frac{\sigma_{s2}}{\sigma_{s1}} = \frac{M_2 C_2 I_1}{M_1 C_1 I_2} \tag{6}$$

where the shell-section moments of inertia are related by

$$\frac{I_2}{I_1} = (\lambda_s^{so})^3 \lambda_s^{st} \tag{7}$$

The ratio of the maximum bending stresses becomes

$$\frac{\sigma_{s2}}{\sigma_{s1}} = \frac{\lambda_{acc}\lambda_h W_{bs}}{(\lambda_s^{so})^2(\lambda_s^{st})} \tag{8}$$

Critical buckling stresses for the shell are related by

$$\frac{\sigma_{sb2}}{\sigma_{sb1}} = \frac{(\lambda_s^{st})^2}{(\lambda_s^{so})^2}\frac{E_{s2}}{E_{s1}} \tag{9}$$

Two additional relationships are assumed by the requirement that buckling and bending stress ratios be equally critical and that the bending-stress ratio be a function of the yield-strength ratio,

$$\frac{\sigma_{sb2}}{\sigma_{sb1}} = \frac{\sigma_{s2}}{\sigma_{s1}} \tag{10}$$

and

$$\frac{\sigma_{s2}}{\sigma_{s1}} = K_s\frac{\sigma_{ys2}}{\sigma_{ys1}} \tag{11}$$

where σ_{ys2} is the yield strength of the shell for array 2, σ_{ys1} is that for array 1, and K_s is the ratio of the factors of safety of the two arrays. These equations (5 through 11) are then solved for the unknowns λ_s^{st}, λ_s^{so}, and W_{bs}, and substituted into Eq. (4).

Table 1 lists the relationships established between the geometric scale factors in Eq. (4) and the ratios of the stresses for all of the components, where

$$W_{bscss} = \frac{W_{bkt2} + W_{s2} + W_{c2} + W_{ss2}}{W_{bkt1} + W_{s1} + W_{c1} + W_{ss1}}$$

$$W_{ba} = \frac{W_{bo2} + W_{a2}}{W_{bo1} + W_{a1}}$$

$$W_{bscssa} = \frac{W_{bkt2} + W_{s2} + W_{c2} + W_{ss2} + W_{a2}}{W_{bkt1} + W_{s1} + W_{c1} + W_{ss1} + W_{a1}}$$

$$\lambda'_h = \frac{\lambda_h \times 7.75 + \lambda_{dia} \times 0.50}{8.25}$$

$$\lambda_{ves} = \left\{ \lambda_v + \left[(\lambda_s^{so})^2 - \lambda_v \right] \frac{r_i^2}{r_o^2} \right\}^{1/2}$$

and

r_i = radius of shell of reference array

r_o = radius of combined shell and rolled blanket for reference array

The equations are then solved for the unknowns λ_s^{so}, λ_s^{st}, λ_c^{st}, λ_{ss}^{so}, λ_{ss}^{st}, λ_{es}^{so}, λ_{es}^{st}, λ_{cs}^{st}, λ_{be}^{so}, λ_{be}^{st}, λ_a^{st}, W_{bs}, W_{bscss}, and W_{ba}. The ratios of the weights of the individual components are then determined by direct substitution of these values into Eq. (4). Table 2 lists the solutions for the above scale factors.

Table 1. Geometric scale factor and stress-level relationships

Ratio	Storage shell	End caps	Support shaft	End supports	Center support	Beam	Actuator
$\frac{M_2}{M_1}$	$\lambda_{acc}\lambda_h W_{bs}$	$\lambda_{acc}(\lambda_s^{so}) W_{bs}$	$\lambda_{acc}\lambda_h W_{bscss}$	$\lambda_{acc}\lambda_{ves} W_{bscss}$	$\lambda_{acc}\lambda_{ves} W_{bscssa}$	$[W_{be}\lambda_{acc}(0.5) + \lambda_t(0.5)]\lambda'_h$	$\lambda_{acc}\lambda_v^{1/2} W_{ba}$
$\frac{\sigma_2}{\sigma_1}$	$\frac{M_2 C_2 I_1}{M_1 C_1 I_2}$	$\frac{M_2 C_2 I_1}{M_1 C_1 I_2}$	$\frac{M_2 C_2 I_1}{M_1 C_1 I_2}$	$\frac{M_2 C_2 I_1}{M_1 C_1 I_2}$	$\frac{M_2 C_2 I_1}{M_1 C_1 I_2}$	$\frac{M_2 C_2 I_1}{M_1 C_1 I_2}$	$\frac{M_2 C_2 I_1}{M_1 C_1 I_2}$
$\frac{I_2}{I_1}$	$(\lambda_s^{so})^3(\lambda_s^{st})$	$(\lambda_s^{so})(\lambda_c^{st})^3$	$(\lambda_{ss}^{so})^3(\lambda_{ss}^{st})$	$(\lambda_{es}^{so})(\lambda_{es}^{st})^3$	$(\lambda_{cs}^{st})^3\lambda_{dia}$	$(\lambda_{be}^{so})^3(\lambda_{be}^{st})$	$\lambda_v(\lambda_a^{st})^2$
$\frac{\sigma_2}{\sigma_1}$	$\frac{\lambda_{acc}\lambda_h W_{bs}}{(\lambda_s^{so})^2(\lambda_s^{st})}$	$\frac{\lambda_{acc} W_{bs}}{(\lambda_c^{st})^2}$	$\frac{\lambda_{acc}\lambda_h W_{bscss}}{(\lambda_{ss}^{so})^2(\lambda_{ss}^{st})}$	$\frac{\lambda_{acc}(\lambda_{ves}) W_{bscss}}{(\lambda_{es}^{so})(\lambda_{es}^{st})^2}$	$\frac{\lambda_{acc}\lambda_{ves} W_{bscssa}}{(\lambda_{cs}^{st})^2\lambda_{dia}}$	$\frac{[W_{be}\lambda_{acc}(0.5) + \lambda_t(0.5)]\lambda'_h}{(\lambda_{be}^{so})^2(\lambda_{be}^{st})}$	$\frac{\lambda_{acc} W_{ba}}{(\lambda_a^{st})^2}$
$\frac{\sigma_{b2}}{\sigma_{b1}}$	$\frac{E_{s2}}{E_{s1}}\left(\frac{\lambda_s^{st}}{\lambda_s^{so}}\right)^2$	—	$\frac{E_{ss2}}{E_{ss1}}\left(\frac{\lambda_{ss}^{st}}{\lambda_{ss}^{so}}\right)^2$	$\frac{E_{es2}}{E_{es1}}\left(\frac{\lambda_{es}^{st}}{\lambda_{es}^{so}}\right)^2$	—	$\frac{E_{be2}}{E_{be1}}\left(\frac{\lambda_{be}^{st}}{\lambda_{be}^{so}}\right)^2$	—

Table 2. Scale-factor solutions for individual components

End caps	Storage shell	Support shaft	Actuator
$\lambda_c^{st} = \left[\frac{\lambda_{acc} W_{bs}}{K_c\left(\frac{\sigma_{yc2}}{\sigma_{yc1}}\right)}\right]^{1/2}$	$\lambda_s^{st} = \left[\lambda_{acc}\lambda_h W_{bs}\left(\frac{E_{s1}}{E_{s2}}\right)\right]^{1/3}$ $\lambda_s^{so} = \left[\frac{\lambda_{acc}\lambda_h W_{bs}}{(\lambda_s^{st}) K_s\left(\frac{\sigma_{ys2}}{\sigma_{ys1}}\right)}\right]^{1/2}$	$\lambda_{ss}^{st} = \left[\frac{\lambda_{acc}\lambda_h W_{bscss}}{\left(\frac{E_{ss2}}{E_{ss1}}\right)}\right]^{1/3}$ $\lambda_{ss}^{so} = \left[\frac{\lambda_{acc}\lambda_h W_{bscss}}{(\lambda_{ss}^{st}) K_{ss}\left(\frac{\sigma_{yss2}}{\sigma_{yss1}}\right)}\right]^{1/2}$	$\lambda_a^{st} = \left[\frac{\lambda_{acc} W_{ba}}{K_a\left(\frac{\sigma_{ya2}}{\sigma_{ya1}}\right)}\right]^{1/2}$

Beam	Center support	End supports
$\lambda_{be}^{st} = \left\{\frac{[W_{be}\lambda_{acc}(0.5) + \lambda_t(0.5)]\lambda'_h}{\left(\frac{E_{be2}}{E_{be1}}\right)}\right\}^{1/3}$ $\lambda_{be}^{so} = \left\{\frac{[W_{be}\lambda_{acc}(0.5) + \lambda_t(0.5)]\lambda'_h}{(\lambda_{be}^{st}) K_{be}\left(\frac{\sigma_{ybe2}}{\sigma_{ybe1}}\right)}\right\}^{1/2}$	$\lambda_{cs}^{st} = \left[\frac{\lambda_{acc}\lambda_{ves} W_{bscssa}}{\lambda_{dia} K_{cs}\left(\frac{\sigma_{ycs2}}{\sigma_{ycs1}}\right)}\right]^{1/2}$	$\lambda_{es}^{st} = \frac{(\lambda_{acc}\lambda_{ves} W_{bscss})^{1/3}}{\left[K_{es}\left(\frac{\sigma_{yes2}}{\sigma_{yes1}}\right)\left(\frac{E_{es2}}{E_{es1}}\right)\right]^{1/6}}$ $\lambda_{es}^{so} = \left[\frac{\lambda_{acc}\lambda_{ves} W_{bscss}}{(\lambda_{es}^{st})^2 K_{es}\left(\frac{\sigma_{yes2}}{\sigma_{yes1}}\right)}\right]$

To determine W_{bs}, W_{bscss}, and W_{ba}, three additional equations (12 through 14) must be written and solved for these three unknowns. To solve these equations, the scale-factor solutions must first be substituted for the scale factors so that the only unknown in each equation is either W_{bs}, W_{bscss}, or W_{ba}:

$$W_{bs} = \frac{W_{bkt1}}{W_{bs1}}\left(\lambda_h \lambda_v \frac{\rho_{bkt2}}{\rho_{bkt1}}\right) + \frac{W_{s1}}{W_{bs1}}\left[\frac{\rho_{s2}}{\rho_{s1}}\left(\lambda_s^{so}\,\lambda_s^{st}\,\lambda_h\right)\right] \tag{12}$$

where W_{bs1} is the weight of the blanket and storage drum shell of the reference array;

$$W_{bscss} = \frac{W_{bs1}}{W_{bscss1}}(W_{bs}) + \frac{W_{c1}}{W_{bscss1}}\left[\frac{\rho_{c2}}{\rho_{c1}}\left(\lambda_s^{so}\right)\left(\lambda_c^{st}\right)^2\right]$$

$$+ \frac{W_{ss1}}{W_{bscss1}}\left[\frac{\rho_{ss2}}{\rho_{ss1}}\left(\lambda_{ss}^{so}\right)\left(\lambda_{ss}^{st}\right)\lambda_h\right] \tag{13}$$

where W_{bscss1} is the weight of the blanket, storage drum shell, end caps, and support shaft of the reference array; and

$$W_{ba} = \frac{W_{bo1}}{W_{ba1}}(W_{bo}) + \frac{W_{a1}}{W_{ba1}}\left(\frac{\rho_{a2}}{\rho_{a1}}\lambda_{dia}\lambda_a^{st}\lambda_v^{1/2}\right) \tag{14}$$

where W_{ba1} is the weight of the boom and the actuator of the reference array. Once these equations have been solved for the W's, and all scale factors have been determined, the final weight is calculated and the power-to-weight ratio is obtained.

This technique for analyzing the size and weight of a structure has inherent limitations. As in all parametric studies, arbitrary decisions have to be made as to how to describe the relationships between load, stress, and member sizes. Because of these limitations, the results obtained from the support-structure analysis are not intended as a substitute for a complete and detailed structural analysis, but as a good initial estimate of the sizing and weight of an array (given a required power output).

IV. Solar Array Parametric Study

The array-optimization and support-structure analyses defined above were used to conduct a parametric analysis to determine the relationships between the performance characteristics of arrays with blanket areas ranging from 100 to 400 ft². This is the range of sizes that is currently receiving the greatest emphasis. Two major results emerged from this study: (1) the determination of the relationship between solar-array weight and the three primary design factors—size, length–width ratio, and deployed natural frequency; (2) a set of plots that provide optimum structural sizing and estimated weights for arrays in the above size range, with widths ranging from 4 to 16 ft, and for deployed natural frequencies ranging from 0.03 to 0.7 Hz.

To limit the scope of the study, certain assumptions had to be made and certain parameters had to be fixed with nominal values. These assumptions must be understood if the parametric plots are to be used effectively:

(1) The analysis is limited to the single-boom, split-blanket configuration, with the boom lying in the plane of the blankets. Because the boom and boom actuator lie in the plane of the blanket, the width available for the blankets is not the total array width; it is the total array width minus the boom-actuator width.

(2) The blanket density is assumed to be 0.17 lb/ft². This density, which corresponds to 8-mil solar cells and 3-mil coverglasses on a 2-mil Kapton substrate, is typical of current designs and is the value used in the baseline design (see Ref. 2). The density is defined by dividing the total blanket area into the total weight of the blankets.

(3) All array-component materials are assumed to be the same as the materials in the baseline design, and all launch-vibration levels are assumed to be equal to the very high levels (1.0 g^2/Hz, 33 g rms) used in the design and testing of the baseline design.

(4) Although the optimum boom-stiffness and blanket-tension determinations are general and apply to all types of booms, the boom was assumed to be a steel BI-STEM with 80% stiffness efficiency and with a boom-diameter-to-material-thickness ratio of 200. This assumption was necessary to generate the plots of component weight, optimum aspect ratio, power-to-weight ratio, and array length vs first-mode natural frequency. The 80% efficiency is based on a degradation of the stiffness of the BI-STEM (two split tubes wrapped around each other) as compared to a closed tube with the same diameter and total wall thickness (the material thickness is one half the total wall thickness) (see Ref. 3).

Use of the parametric plots for arrays that violate these assumptions should be done carefully. For example, change of the blanket density affects the array parameters considerably, whereas change to a different boom efficiency or diameter-to-thickness ratio does not affect them significantly, and the plots may be used.

In the preliminary design of roll-up solar arrays, the most important parameter for obtaining the optimum array is the determination of the optimum aspect ratio (total array length/total array width). This optimum aspect ratio has been found to be essentially independent of array size; thus, for fixed blanket and base-structure parameters, it is only a function of the required first-mode natural frequency. Figure 6 is a typical graph of component weights vs natural frequency of an array using two different aspect ratios. It can be seen that, at low first-mode natural frequencies, the 8/1 aspect ratio requires less total system weight and thus has a higher power-to-weight ratio than has the 2/1 aspect ratio. The reason for the lower total system weight of the 8/1 aspect ratio array is that, for narrow array widths, the required size and weight of the storage drum and related base components are less than they are for wide array widths, whereas, at low natural-frequency requirements, the long boom is still relatively lightweight and the boom actuator is still relatively small. However, for requirements of higher natural frequencies, the long boom increases in size and weight at such a rapid rate (to meet the increased stiffness requirements) that the smaller aspect ratios become more efficient because the shorter boom increases in size and weight at a much slower rate as the required natural frequency increases. The empirically derived relationship between optimum aspect ratio and deployed natural frequency for the blanket density and base-structure parameters used in this study is shown in Fig. 7.

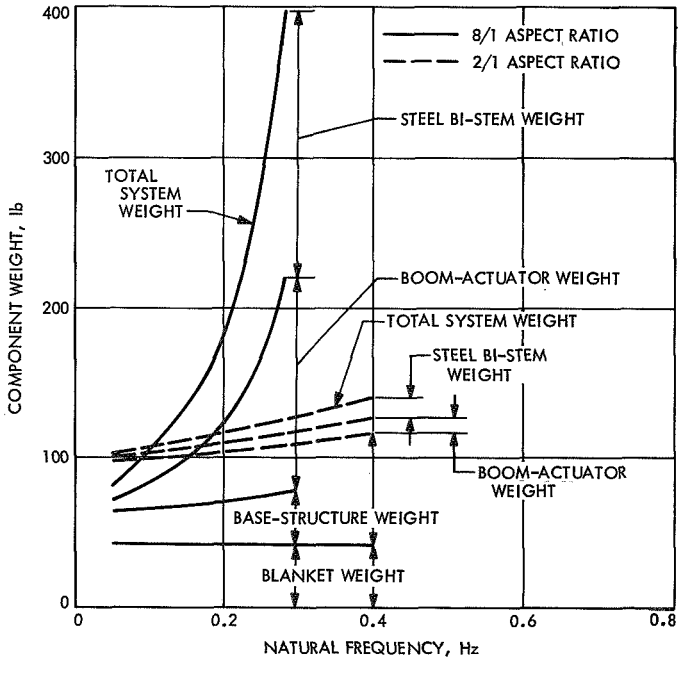

Fig. 6. Dependence of component weights on natural frequency and array aspect ratio for a typical 250-ft², BI-STEM boom array

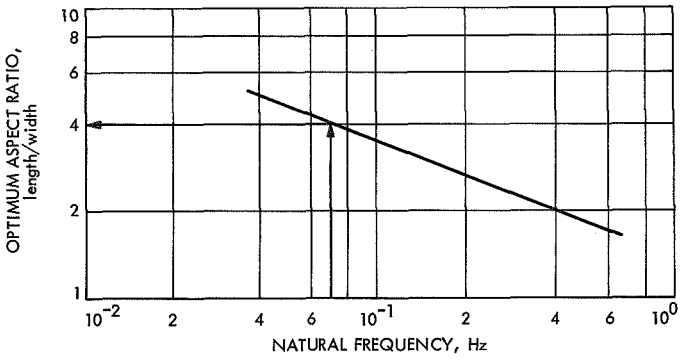

Fig. 7. Optimum aspect ratio for any size array as a function of deployed natural frequency

By using Figs. 7 through 10, which are typical of those found in Appendix A, a user with a required array area can determine the values of all of the major design parameters of a roll-up solar array, including length, total width, power-to-weight ratio, boom stiffness, and blanket tension. A typical design of a solar array will be carried out in Section V to describe the use of the parametric curves in Appendix A.

V. Use of Parametric Curves

When it is desired to determine the overall dimensions of a proposed array, Figs. 7 and 8 can be used together to determine the desired aspect ratio. As a typical example, a natural frequency requirement of 0.07 Hz for a 250-ft² array will be considered. From Fig. 7, it is determined that the optimum aspect ratio for 0.07 Hz is approximately 4/1. This gives a total width and length slightly greater than 8 and 32 ft, respectively. Although the total width and length produce an area greater than 250 ft², the added width and length are required to compensate for the lost area between the two split blankets. This area is occupied by the boom and the boom actuator.

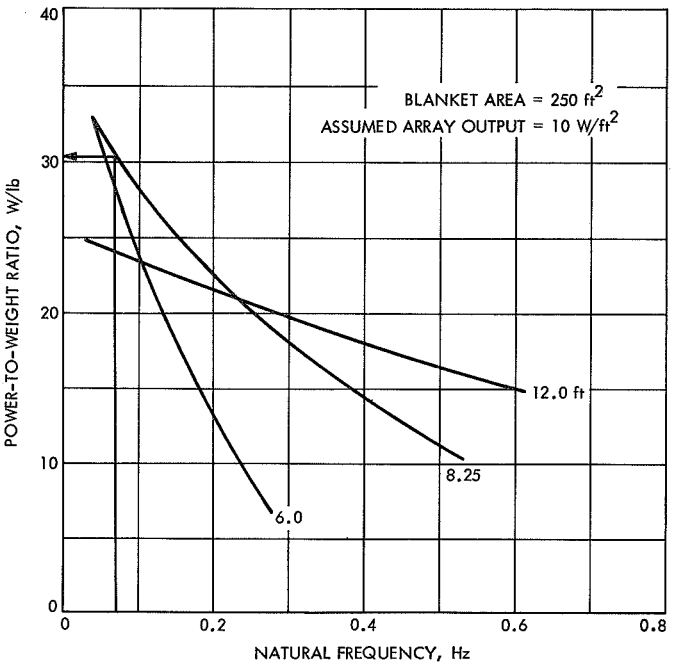

Fig. 8. Typical dependence of power-to-weight ratio on deployed natural frequency for various array widths

In Fig. 8, which is the plot of power-to-weight ratio for a 250-ft² array, the curve for the 8.25-ft width is used to determine the appropriate power-to-weight ratio at the natural frequency of 0.07 Hz. The value obtained is found to be slightly greater than 30 W/lb, based on 10-W/ft² array output. If the array output is different from the assumed value (say, X W/ft²), the actual efficiency can be obtained from

$$(\text{power-weight})_{\text{actual}} = [(\text{power/weight})_{\text{curve}}] \times \left(\frac{X \text{ W/ft}^2}{10 \text{ W/ft}^2}\right)$$

If the width or length of the array is limited by design constraints to values other than the optimum, the decrease in power-to-weight ratio associated with size variations from the optimum is given in Fig. 8. For example, with a 6-ft width, the power-to-weight ratio at 0.07 Hz drops from 30.5 to 28 W/lb.

Once the overall dimensions have been ascertained, the optimum boom stiffness and optimum blanket tension can be determined by use of Fig. 9. From this figure, it can be seen that, as the natural frequency requirement increases, the optimum boom stiffness and optimum blanket tension increase rapidly, thus decreasing the power-to-weight efficiency of the overall array. At 0.10 Hz, only a 3300-lb-ft² boom stiffness and a tension of 3.4 lb per blanket are required for a 250-ft² array. However, the same array requires a 100,000-lb-ft² boom stiffness and a tension of 60 lb per blanket at 0.40 Hz. By use of the example given above (0.07 Hz and 250 ft²), it can be determined from Fig. 9 (solid line) that the optimum boom stiffness required is 1600 lb-ft² and the corresponding tension is 1.8 lb per blanket. The blanket-tension curves in Fig. 9 all stop at approximately 2 lb, which corresponds to a minimum allowable wrap force of approximately 0.5 lb/ft (of width); this force is needed to roll the blanket on the storage drums.

Although the optimum boom-stiffness curve is general and can be used for any type of boom, the boom mass used in the modal analysis program was the mass of a steel BI-STEM boom with 80% stiffness efficiency and a diameter-to-thickness ratio of 200. When the optimum boom-stiffness curves are used for booms other than the assumed boom, there will be a discrepancy between the predicted first-mode natural frequency and the actual frequency because of the different boom mass-to-stiffness ratio. At low natural frequencies, when the boom weight is small compared to the blanket weight, these discrepancies will be negligible; at high natural frequencies, however, when the boom weight is very large, the deviations can be significant, depending upon the magnitude of the differences in the respective mass-to-stiffness ratios.

If the optimum boom stiffness obtained is not that of a standard, off-the-shelf size of boom, then Fig. 9 can be used to determine the natural frequency and optimum blanket tension for an available boom stiffness. If 2000 lb-ft² is assumed as the stiffness of an off-the-shelf boom near the optimum, the dotted lines in Fig. 9 represent the determination of the first-mode natural frequency and optimum tension. The natural frequency obtained is 0.08 Hz and the tension is 2.2 lb per blanket.

Figure 10 is a typical plot of array length vs first-mode natural frequency. Given a required blanket area and specified total array width, the overall length becomes greater as the first-mode natural frequency increases. This increase in length is required to compensate for the decrease in array width available for the blankets caused by the increase in actuator width between blankets. The actuator-width increase is caused by an increase in required boom stiffness and diameter at high natural frequencies. For high aspect ratio and relatively narrow arrays, this phenomenon becomes more evident because the actuator width requires a larger

percentage of the total available array width. In Fig. 10, the effect of the different aspect ratios on change in length is shown. For a 400-ft² array at 0.03 Hz, the length is 51.5 ft; at 0.3 Hz, the same 400-ft² array requires 67.5 ft. At low aspect ratios, this length increase is small and the increase in stiffness needed to compensate for the small change in length is negligible. Thus, the low-aspect-ratio curves are essentially linear. By use of the data shown in Fig. 10, an example array 250 ft², 8.25 ft wide, at 0.07 Hz requires a length of 32 ft.

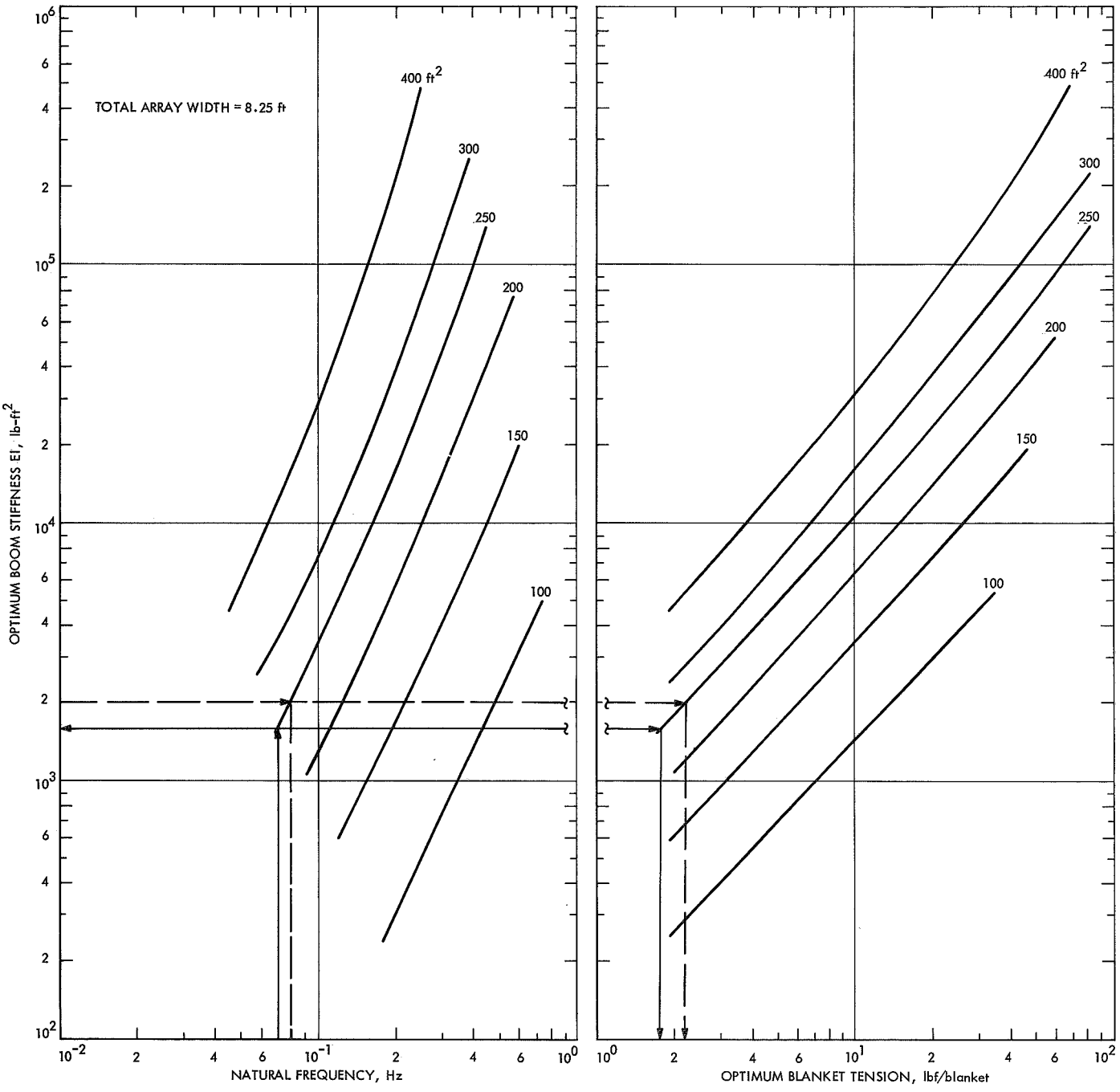

Fig. 9. Optimum boom stiffness and blanket tension vs deployed natural frequency and blanket area for a typical array width

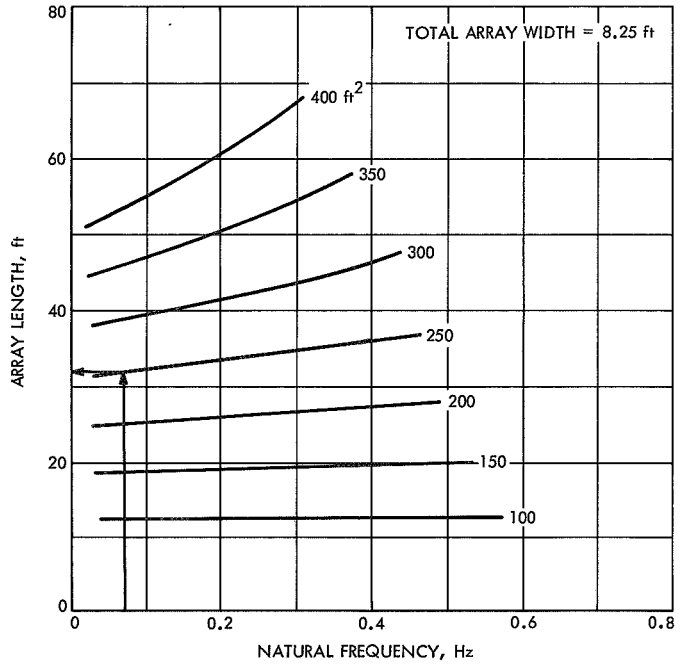

Fig. 10. Variation in array length with deployed natural frequency caused by increase in boom length and actuator width with increasing boom stiffness for a typical steel BI-STEM boom with $D/t = 200$ and 80% efficiency

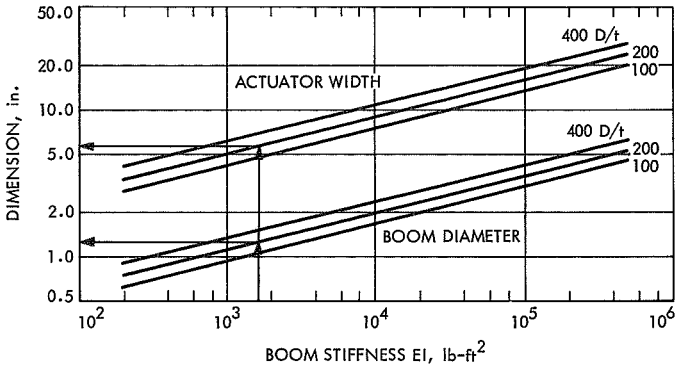

Fig. 11. Boom diameter and boom-actuator width as a function of bending stiffness for a steel BI-STEM element (assuming 80% efficiency)

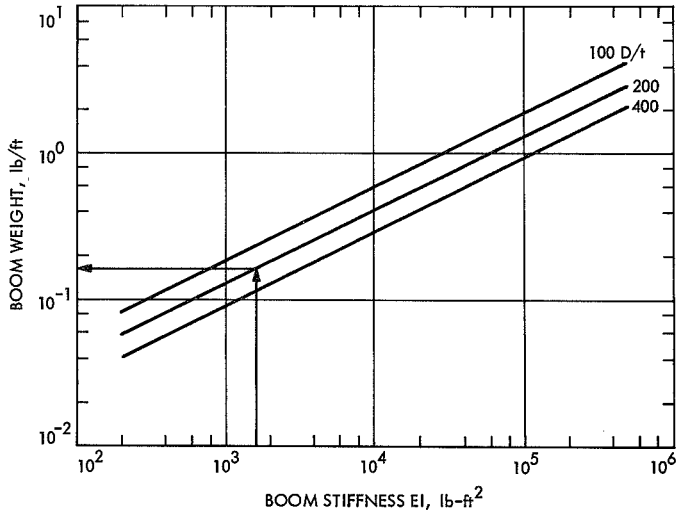

Fig. 12. Weight per foot vs bending stiffness for a steel BI-STEM boom element (assuming 80% efficiency)

Once the required boom stiffness has been determined, the sizing of the boom is simply a calculation of the diameter and thickness needed to obtain the required moment of inertia (given the boom-material modulus of elasticity). Figures 11 and 12 are plots of these calculations for a typical steel BI-STEM of 80% efficiency. Figure 11 is a plot of boom diameter and actuator width vs boom stiffness for various D/t (diameter/thickness) ratios. This curve shows the direct relationship between the actuator width and boom diameter. The value of the boom stiffness for the design of the example has been drawn on the curve, and the boom diameter and actuator width were found to be 1.26 and 5.6 in., respectively. By use of Fig. 12, the boom weight for the example array is 0.16 lb/ft (of length).

In this report, one of the major design parameters that has not been considered in depth is the variation of blanket density and its effect on other parameters. Blanket density affects all parameters, including optimum aspect ratio; therefore, to develop a set of parametric plots for varying blanket density would require a complete set of plots similar to those in Appendix A for each density variation.

Figures 13 and 14 show two typical parameter variations of a 250-ft² array at various blanket densities. Figure 13 shows the effect of blanket density on power-to-weight ratio. The significant difference in power-to-weight ratio at different blanket densities results not only from the different blanket weights, but from a change in weight of related structural components. As the blanket weight increases or decreases, significant increases or decreases are required in the boom, the boom actuator, and the related base structure. Figure 14 shows this large variation in boom stiffness that is required to compensate for the change in blanket weight. If the blanket density is doubled, the boom stiffness must be approximately doubled to maintain the required frequency.

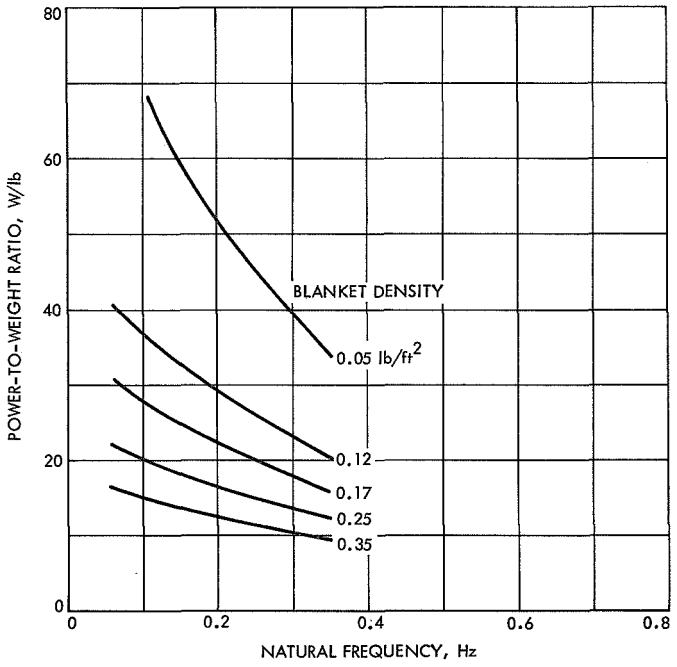

Fig. 13. Dependence of solar-array efficiency on blanket weight per unit area for a typical 8.25-ft wide, 250-ft² area, 10-W/ft² output, steel BI-STEM boom array

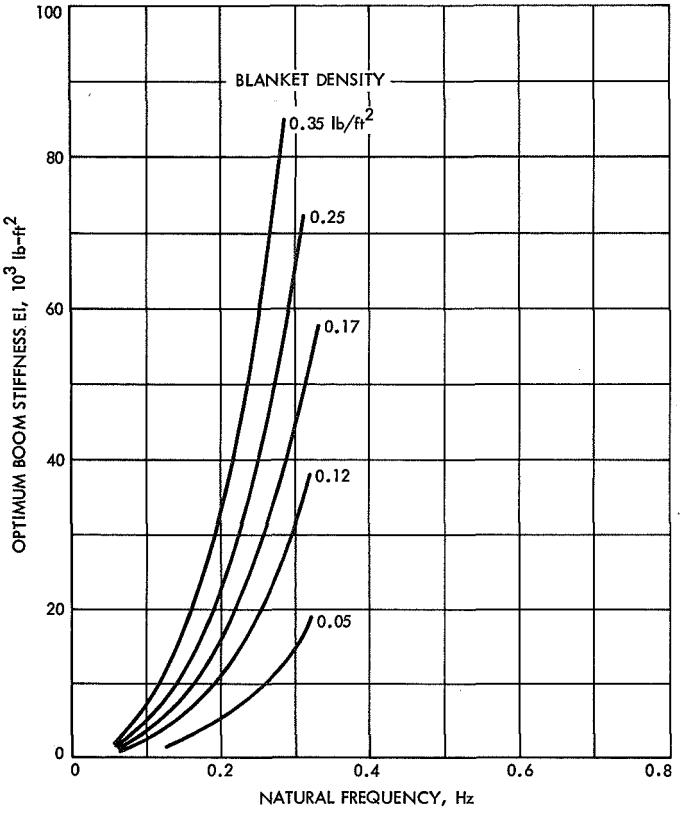

Fig. 14. Dependence of optimum (minimum) boom stiffness on blanket weight per unit area for a typical 8.25-ft wide, 250-ft² area, 10-W/ft² output, steel BI-STEM boom array

VI. Conclusion

The catalog of parametric plots contained in Appendix A, together with the computer program developed in this study, provides a ready means of evaluating the performance characteristics of contemplated new designs for roll-up solar arrays based on the engineering prototype (see Ref. 2). By use of these plots, a quick evaluation of the potential merits of a proposed roll-up solar array can be made. Although the parametric plots have required assumptions that limit their generality, the computer program is sufficiently general to accept all single-boom, split-blanket configurations, and is able to determine the implications of overall geometric scaling, aspect ratio scaling, inertial load scaling, and changes in structural materials.

The roll-up solar array analysis program is an efficient tool for the modal analysis of a deployed solar array. The speed of the finite-element procedure and eigenvalue determination, combined with the rapid convergence of the optimization routines, produces a highly efficient program for the determination of optimum boom stiffness and blanket tension; an optimum (lowest-weight) boom can thus be designed. The modal-analysis program has been found to be more accurate in the determination of the first modes of vibration than the method of lumped masses on vibrating strings. Although the membrane finite element does not include any bending stiffness, additional work has been done by refining this element to include the stiffness effect. It was found that, although the bending stiffness had an effect on higher modes of vibration, the first symmetric and antisymmetric modes were unaffected.

The modal-analysis results obtained compare favorably with the results of tests that have been run on the existing prototype (see Ref. 2). The roll-up solar array analysis program is also an effective tool for obtaining preliminary weight, sizes, overall efficiencies, and frequencies that can be compared to the weight and frequencies of other types of arrays (fold-up, rigid panels, etc.). The results obtained from support-structure analysis are not intended as a substitute for a complete and detailed structural analysis; they are intended as an effective means of predicting the performance characteristics of proposed array sizes that vary from the engineering prototype in size.

References

1. Martin, H. C., "On the Derivation of Stiffness Matrices for the Analysis of Large Deflection and Stability Problems," in *Proceedings of the Conference on Matrix Methods Structural Mechanics, Wright Patterson Air Force Base, Ohio, October 26–28, 1965.* AFFDL Technical Report 66-80, pp. 697–716, 1966. Clearing House for Federal Scientific and Technical Information, Springfield, Va.

2. *Final Report, Design and Development of a 30 Watts per Pound, 250 Square Foot Roll-Up Solar Array,* Document 70SD4286. Prepared for the Jet Propulsion Laboratory by the Missiles and Space Division, General Electric Co., Philadelphia, Pa., Dec. 1, 1970.

3. *Study of Deployment/Retraction Techniques for Flexible, Roll-Up Solar Arrays,* Document 834FR3001. Prepared for Marshall Space Flight Center by Space and Electronics Systems Division, Fairchild Hiller Corp., Germantown, Md., Jan. 31, 1969.

Appendix A

Parametric Plots

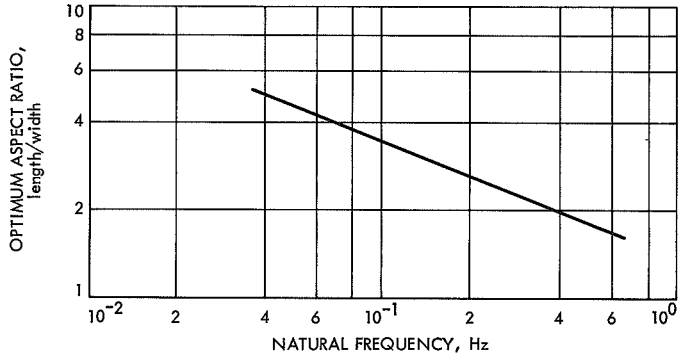

Fig. A-1. Optimum aspect ratio for any size array as a function of deployed natural frequency

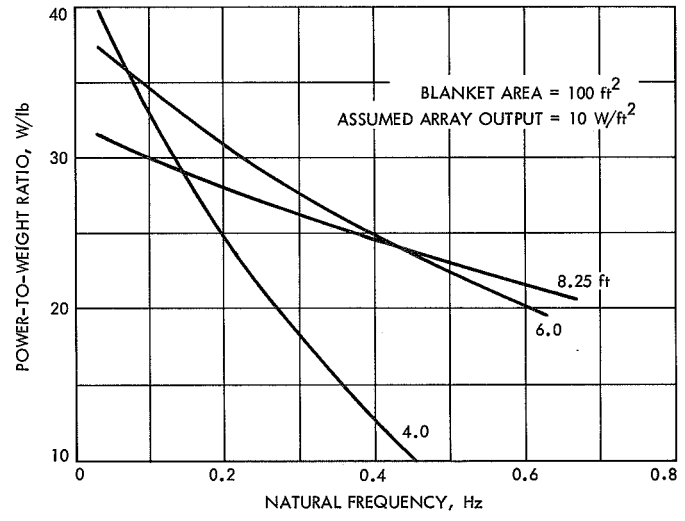

Fig. A-2. Dependence of power-to-weight ratio upon deployed natural frequency for various array widths (100-ft² blanket area)

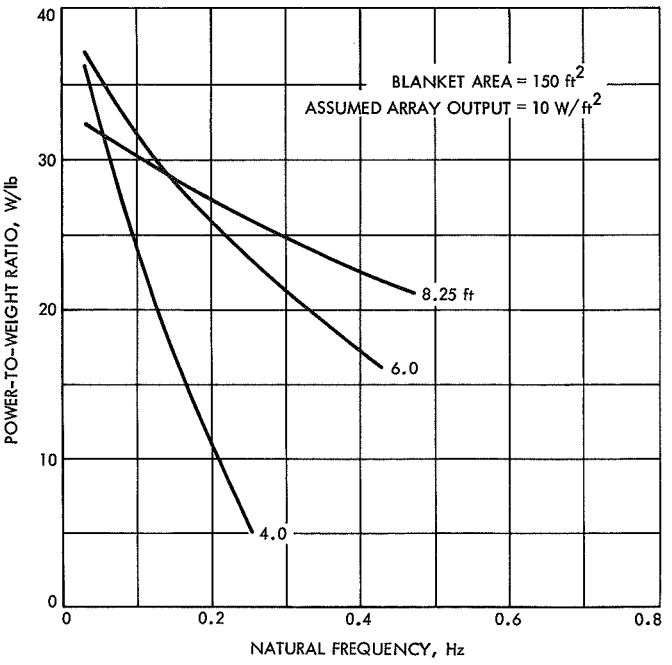

Fig. A-3. Dependence of power-to-weight ratio upon deployed natural frequency for various array widths (150-ft² blanket area)

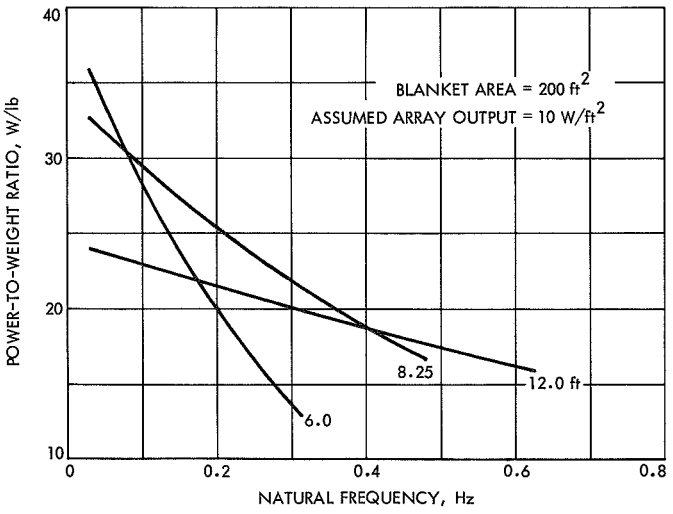

Fig. A-4. Dependence of power-to-weight ratio upon deployed natural frequency for various array widths (200-ft² blanket area)

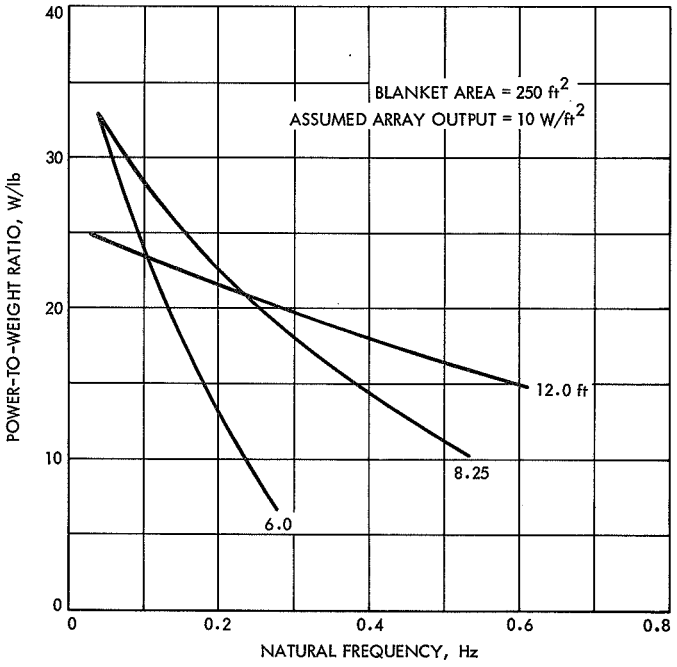

Fig. A-5. Dependence of power-to-weight ratio upon deployed natural frequency for various array widths (250-ft² blanket area)

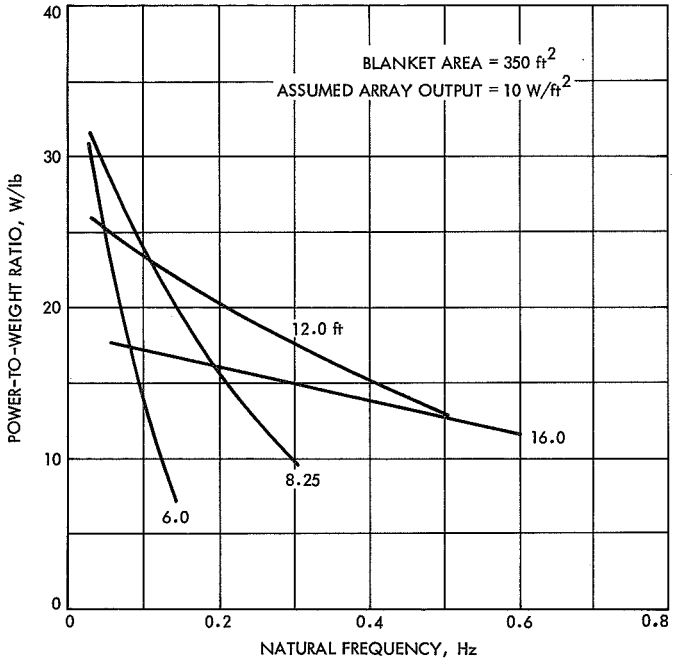

Fig. A-7. Dependence of power-to-weight ratio upon deployed natural frequency for various array widths (350-ft² blanket area)

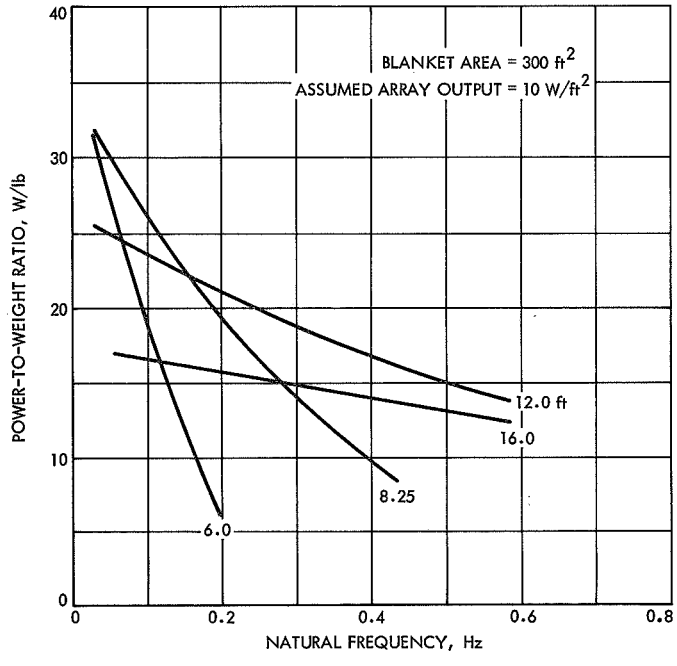

Fig. A-6. Dependence of power-to-weight ratio upon deployed natural frequency for various array widths (300-ft² blanket area)

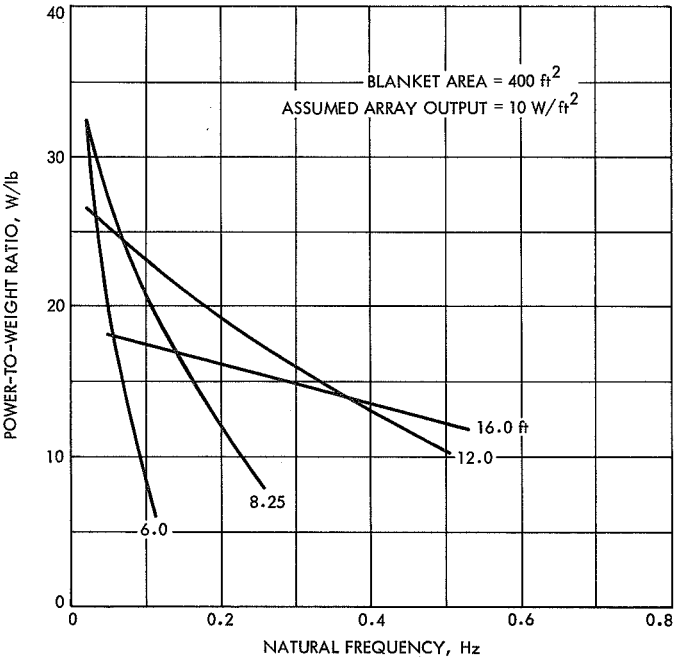

Fig. A-8. Dependence of power-to-weight ratio upon deployed natural frequency for various array widths (400-ft² blanket area)

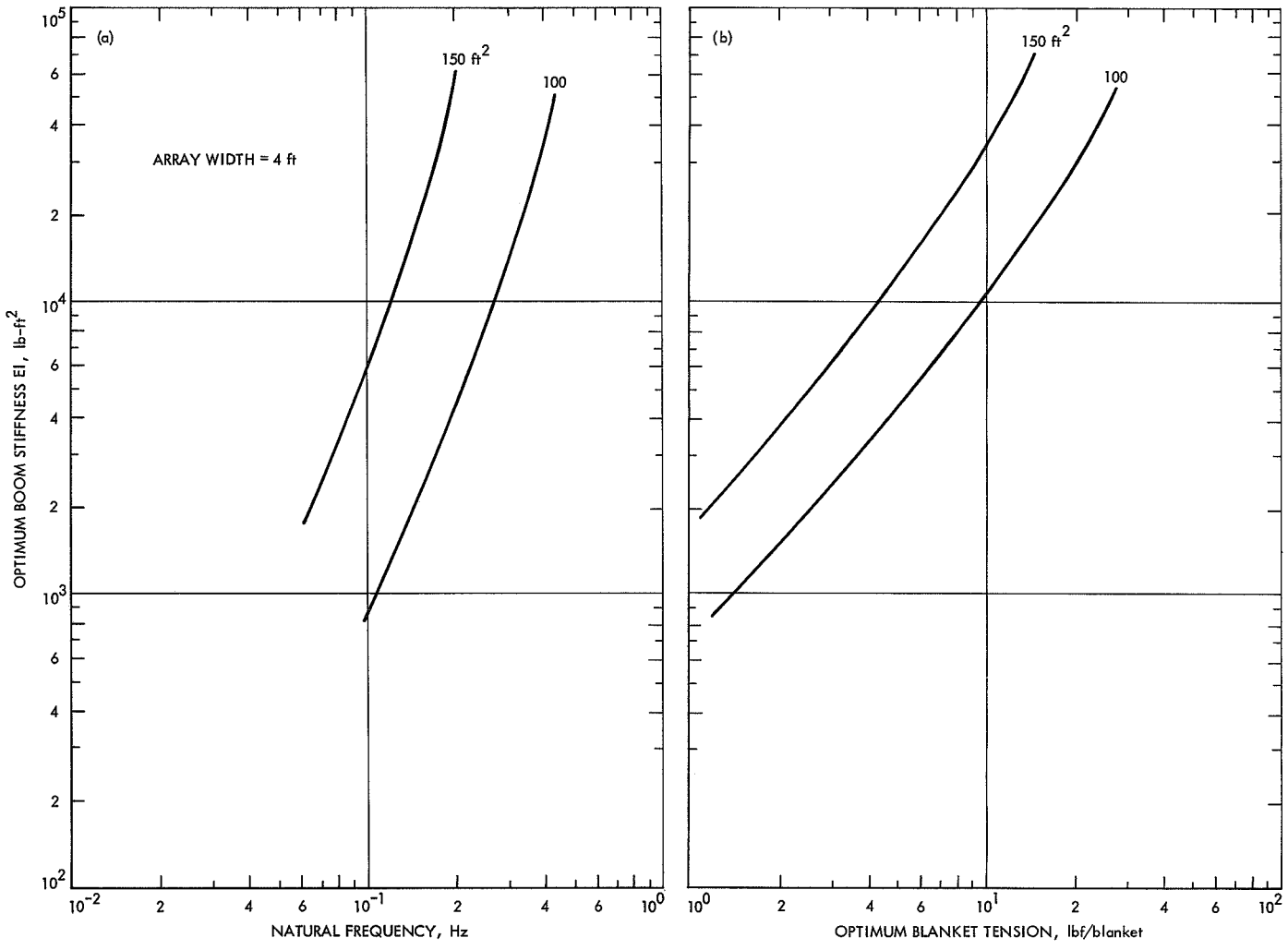

Fig. A-9. Optimum boom stiffness for a 4-ft-wide array: (a) optimum boom stiffness vs deployed natural frequency and blanket area; (b) optimum boom stiffness vs optimum blanket tension and blanket area

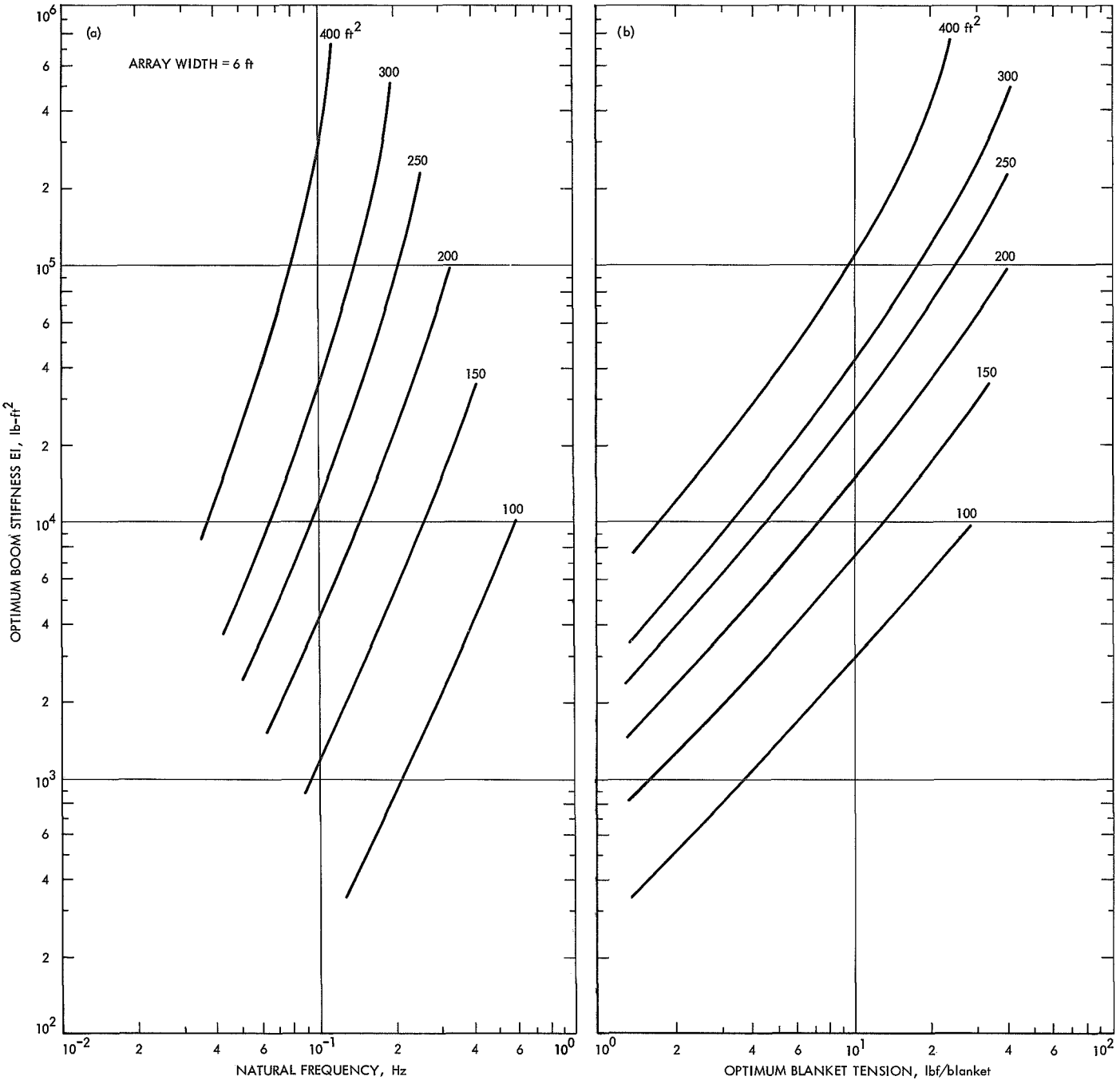

Fig. A-10. Optimum boom stiffness for a 6-ft-wide array: (a) optimum boom stiffness vs deployed natural frequency and blanket area; (b) optimum boom stiffness vs optimum blanket tension and blanket area

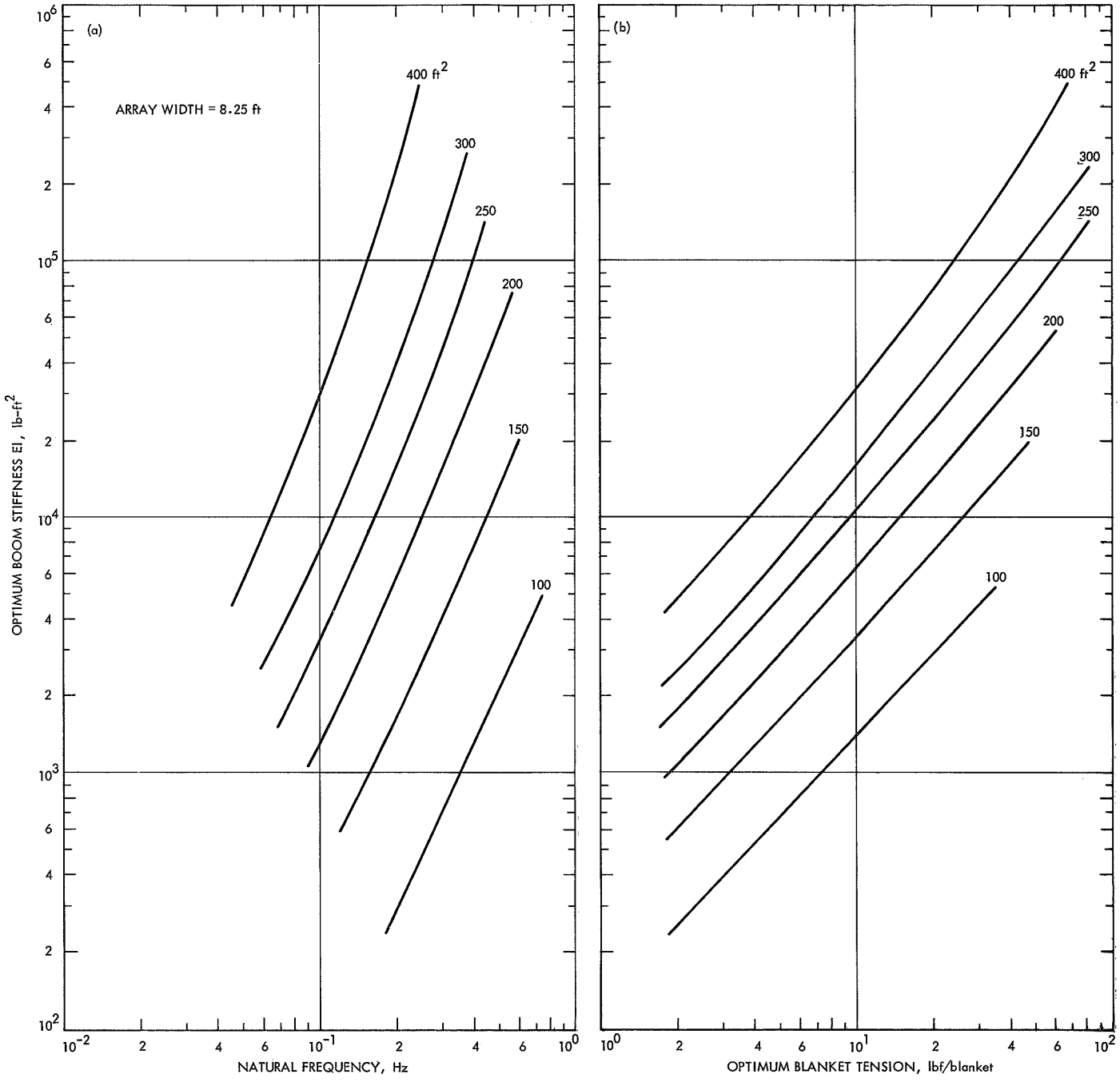

Fig. A-11. Optimum boom stiffness for an 8.25-ft-wide array: (a) optimum boom stiffness vs deployed natural frequency and blanket area; (b) optimum boom stiffness vs optimum blanket tension and blanket area

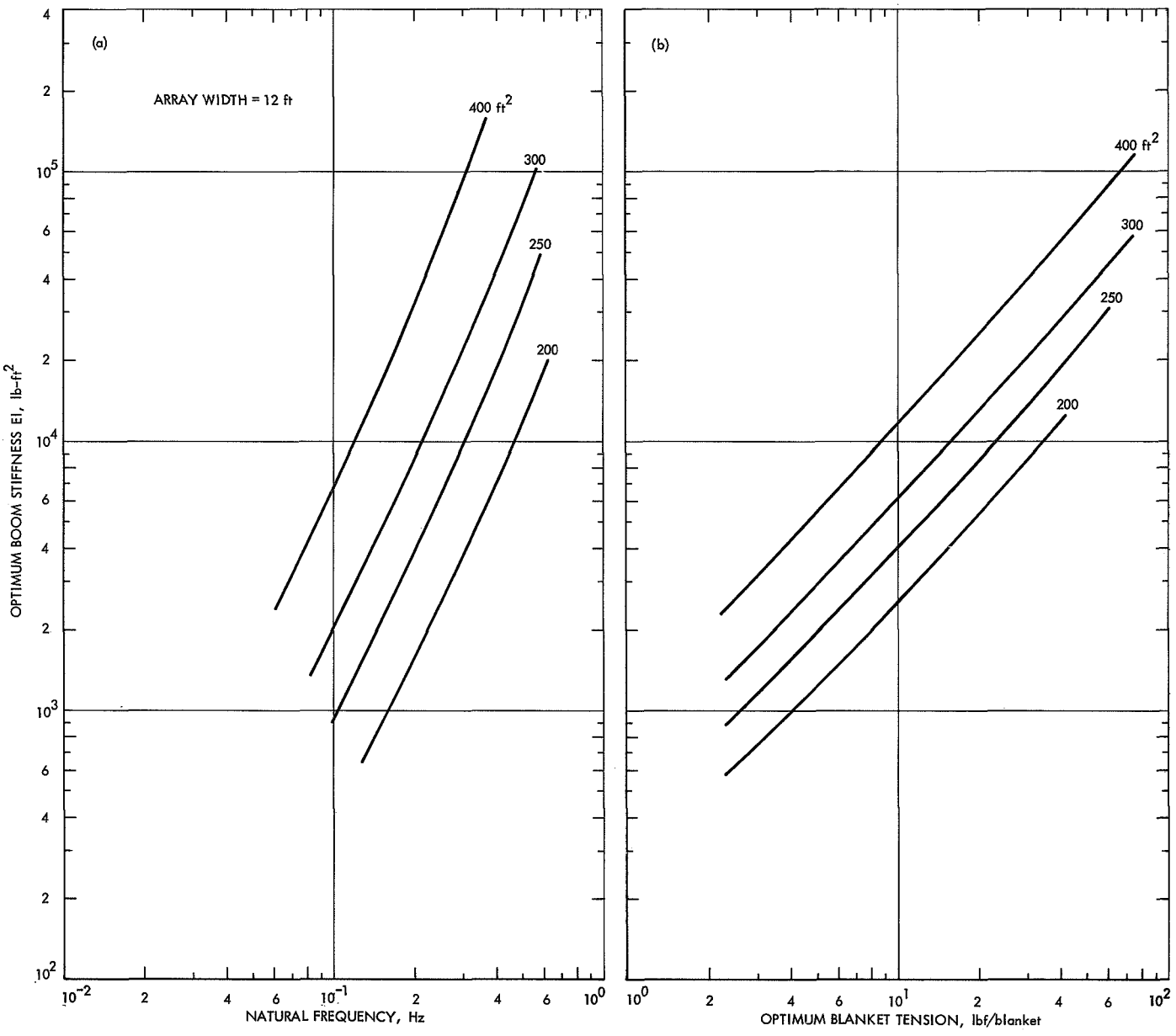

Fig. A-12. Optimum boom stiffness for a 12-ft-wide array: (a) optimum boom stiffness vs deployed natural frequency and blanket area; (b) optimum boom stiffness vs optimum blanket tension and blanket area

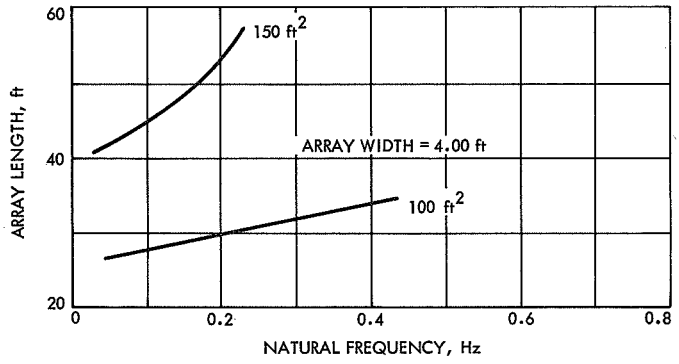

Fig. A-13. Array length vs deployed natural frequency and blanket area for a 4-ft-wide array

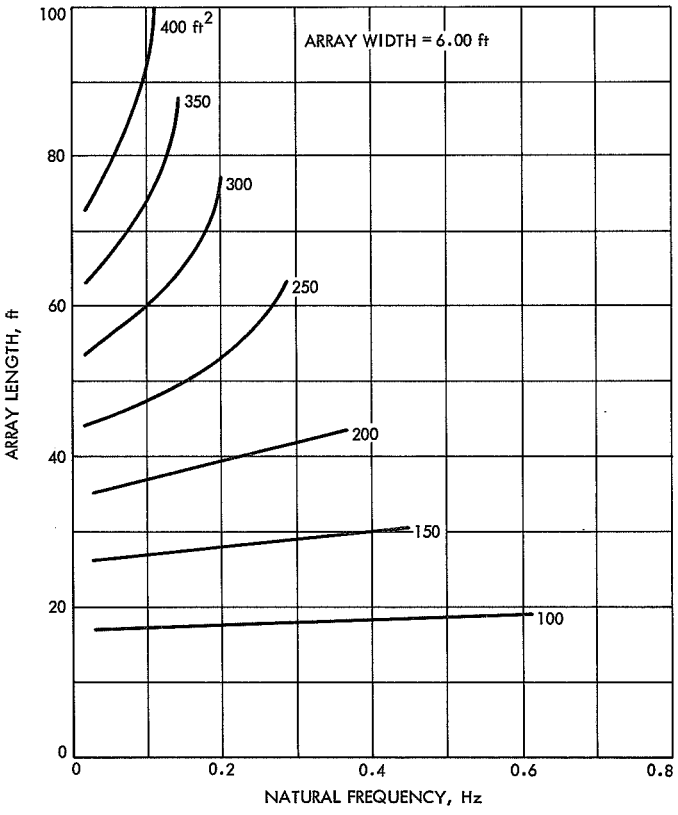

Fig. A-14. Array length vs deployed natural frequency and blanket area for a 6-ft-wide array

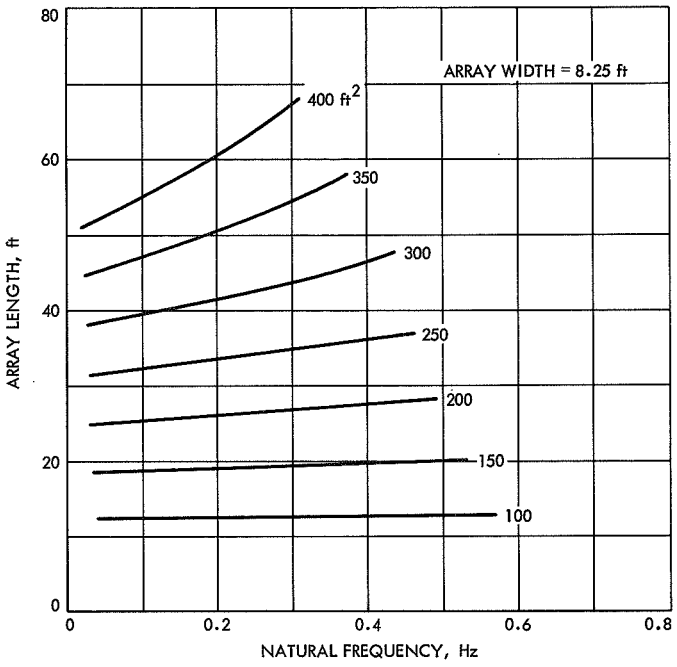

Fig. A-15. Array length vs deployed natural frequency and blanket area for an 8.25-ft-wide array

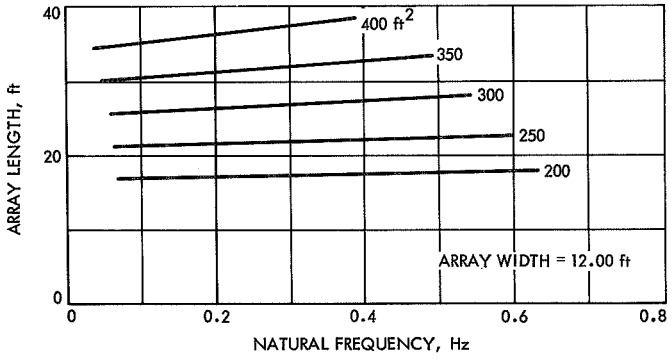

Fig. A-16. Array length vs deployed natural frequency and blanket area for a 12-ft-wide array

Appendix B

Elemental Stiffness and Consistent Mass Matrices for Blanket and Beam Elements

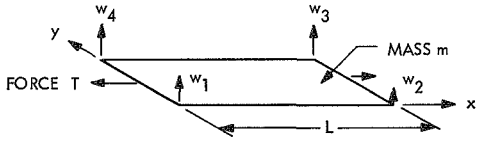

$$K = \frac{T}{L}\begin{bmatrix} w_1 & w_2 & w_3 & w_4 \\ 1/3 & & & \text{SYM} \\ -1/3 & 1/3 & & \\ -1/6 & 1/6 & 1/3 & \\ 1/6 & -1/6 & -1/3 & 1/3 \end{bmatrix} \qquad M = m\begin{bmatrix} w_1 & w_2 & w_3 & w_4 \\ 1/9 & & & \text{SYM} \\ 1/18 & 1/9 & & \\ 1/36 & 1/18 & 1/9 & \\ 1/18 & 1/36 & 1/18 & 1/9 \end{bmatrix}$$

Fig. B-1. Rectangular membrane finite element

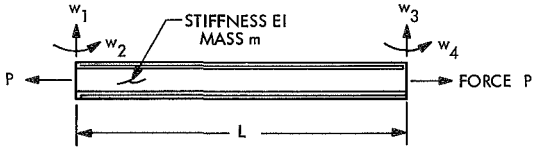

$$K = \frac{2EI}{L^3}\begin{bmatrix} w_1 & w_2 & w_3 & w_4 \\ 6 & & & \text{SYM} \\ 3L & 2L^2 & & \\ -6 & -3L & 6 & \\ 3L & L^2 & -3L & 2L^2 \end{bmatrix} + \frac{P}{5}\begin{bmatrix} w_1 & w_2 & w_3 & w_4 \\ 6/L & & & \text{SYM} \\ 1/2 & 2L/3 & & \\ -6/L & -1/2 & 6/L & \\ 1/2 & -L/6 & -1/2 & 2L/3 \end{bmatrix}$$

$$M = \frac{m}{420}\begin{bmatrix} w_1 & w_2 & w_3 & w_4 \\ 156 & & & \text{SYM} \\ 22L & 4L^2 & & \\ 54 & 13L & 156 & \\ -13L & -3L^2 & -22L & 4L^2 \end{bmatrix}$$

Fig. B-2. Beam column finite element

NASA — JPL — Coml., L.A., Calif.

N71-13427

TECHNICAL REPORT STANDARD TITLE PAGE

1. Report No. 32-1502	2. Government Accession No.	3. Recipient's Catalog No.
4. Title and Subtitle PARAMETRIC STUDY OF THE PERFORMANCE CHARACTERISTICS AND WEIGHT VARIATIONS OF LARGE-AREA ROLL-UP SOLAR ARRAYS		5. Report Date December 15, 1970 6. Performing Organization Code
7. Author(s) J. V. Coyner, Jr., R. G. Ross, Jr.		8. Performing Organization Report No.
9. Performing Organization Name and Address JET PROPULSION LABORATORY California Institute of Technology 4800 Oak Grove Drive Pasadena, California 91103		10. Work Unit No. 11. Contract or Grant No. NAS 7-100 13. Type of Report and Period Covered Technical Report
12. Sponsoring Agency Name and Address NATIONAL AERONAUTICS AND SPACE ADMINISTRATION Washington, D.C. 20546		14. Sponsoring Agency Code

15. Supplementary Notes

16. Abstract

An analysis has been conducted to determine the relationships between the performance characteristics (power-to-weight ratio, blanket tension, structural member section dimensions, and resonant frequencies) of large-area roll-up solar arrays of the single-boom, tensioned-substrate design. The study includes the determination of the size and weight of the base structure supporting the boom and blanket and the determination of the optimum width, blanket tension, and deployable boom stiffness needed to achieve the minimum-weight design for a specified frequency for the first mode of vibration. A computer program has been used to generate a set of plots that provide optimum structural sizing and estimated weights for arrays with blanket areas ranging from 100 to 400 ft^2 and for first-mode natural frequencies ranging from 0.03 to 0.7 Hz. Use of these plots enables a quick evaluation of the potential merits of a proposed roll-up array.

17. Key Words (Selected by Author(s))	18. Distribution Statement
Power Sources Structural Engineering	Unclassified -- Unlimited

19. Security Classif. (of this report)	20. Security Classif. (of this page)	21. No. of Pages	22. Price
Unclassified	Unclassified	23	

HOW TO FILL OUT THE TECHNICAL REPORT STANDARD TITLE PAGE

Make items 1, 4, 5, 9, 12, and 13 agree with the corresponding information on the report cover. Use all capital letters for title (item 4). Leave items 2, 6, and 14 blank. Complete the remaining items as follows:

3. Recipient's Catalog No. Reserved for use by report recipients.

7. Author(s). Include corresponding information from the report cover. In addition, list the affiliation of an author if it differs from that of the performing organization.

8. Performing Organization Report No. Insert if performing organization wishes to assign this number.

10. Work Unit No. Use the agency-wide code (for example, 923-50-10-06-72), which uniquely identifies the work unit under which the work was authorized. Non-NASA performing organizations will leave this blank.

11. Insert the number of the contract or grant under which the report was prepared.

15. Supplementary Notes. Enter information not included elsewhere but useful, such as: Prepared in cooperation with... Translation of (or by)... Presented at conference of... To be published in...

16. Abstract. Include a brief (not to exceed 200 words) factual summary of the most significant information contained in the report. If possible, the abstract of a classified report should be unclassified. If the report contains a significant bibliography or literature survey, mention it here.

17. Key Words. Insert terms or short phrases selected by the author that identify the principal subjects covered in the report, and that are sufficiently specific and precise to be used for cataloging.

18. Distribution Statement. Enter one of the authorized statements used to denote releasability to the public or a limitation on dissemination for reasons other than security of defense information. Authorized statements are "Unclassified—Unlimited," "U. S. Government and Contractors only," "U. S. Government Agencies only," and "NASA and NASA Contractors only."

19. Security Classification (of report). NOTE: Reports carrying a security classification will require additional markings giving security and downgrading information as specified by the Security Requirements Checklist and the DoD Industrial Security Manual (DoD 5220.22-M).

20. Security Classification (of this page). NOTE: Because this page may be used in preparing announcements, bibliographies, and data banks, it should be unclassified if possible. If a classification is required, indicate separately the classification of the title and the abstract by following these items with either "(U)" for unclassified, or "(C)" or "(S)" as applicable for classified items.

21. No. of Pages. Insert the number of pages.

22. Price. Insert the price set by the Clearinghouse for Federal Scientific and Technical Information or the Government Printing Office, if known.